EPR Theoretical Study of the Local Lattice Structure of Fe^{3+} Doped in $MgTiO_3$ and $LiTaO_3$

Lei-Lei Pan[a], Xiao-Yu Kuang[a,b], Guang-Dong Li[a], and Hui Wang[a]

[a] Institute of Atomic and Molecular Physics, Sichuan University, Chengdu 610065, China
[b] International Centre for Materials Physics, Academia Sinica, Shenyang 110016, China

Reprint requests to X.-Y. K.; E-mail: panlei225@163.com

Z. Naturforsch. **62a,** 101 – 106 (2007); received November 9, 2006

The EPR zero-field splittings of Fe^{3+} doped in $MgTiO_3$ and $LiTaO_3$ are studied by diagonalizing the complete energy matrices of the electron-electron repulsion, ligand-field and spin-orbit coupling interactions for a d^5 configuration ion in a trigonal ligand-field. It is shown that, when Fe^{3+} is doped in a $MgTiO_3$ or $LiTaO_3$ crystal, the local lattice structure around the octahedral Fe^{3+} center has an obvious distortion along the C_3 axis. By simulating the second- and fourth-order EPR parameters D and $(a-F)$ simultaneously, the local structure parameters of Fe^{3+} doped in $MgTiO_3$ and $LiTaO_3$ crystals are determined, which reveal that Fe^{3+} occupies both the Mg^{2+} and Ti^{4+} sites in the $MgTiO_3$:Fe^{3+} system and occupies the Li^+ site rather than the Ta^{5+} site in the $LiTaO_3$:Fe^{3+} system. The results accord with the ENDOR and EPR experiments. – PACS numbers: 71.70.Gm; 75.30.Et; 71.70.Ch.

Key words: $MgTiO_3$:Fe^{3+} and $LiTaO_3$:Fe^{3+} Systems; Local Lattice Structure; EPR Spectrum.

1. Introduction

The ABO_3 type (A = Mg, Li, K, La; B = Ti, Ta, Nb, Al) pervoskite structure is one of the typical structures of ion crystals, which are extensively applied in the industry [1, 2]. $MgTiO_3$ and $LiTaO_3$ crystals, belonging to the ABO_3 type like Al_2O_3 [3], are important dielectric materials. Their crystals, doped with Fe^{3+} are of great interest because of their application in ceramic multilayer capacitors, electro-optic, waveguide and nonlinear optical devices [4 – 6]. In particular, the impurity ion Fe^{3+} plays an important role in the photorefractive effect [7]. Therefore, it is necessary to know the local lattice structure of the impurity centers. From ENDOR and EPR experiments [8 – 10, 15], one knows that Fe^{3+}, doped in $MgTiO_3$ crystals, replaces both Mg^{2+} and Ti^{4+} sites, and their zero-field splitting parameters were measured on the basis of the angular dependence of EPR spectra. As for Fe^{3+} doped in $LiTaO_3$, according to the EPR parameter D [8 – 16], it replaces the Li^+ site rather than the Ta^{5+} site. Until now, however one can not explain satisfactorily the interrelation between the local lattice structure and the EPR spectrum of Fe^{3+} doped in $MgTiO_3$ and $LiTaO_3$ crystals.

It is well known that for a d^5 configuration ion in a trigonal ligand-field the high-spin ground-state is the $^6A_1$ state. In order to describe the $^6A_1$ ground state splitting, the spin Hamiltonian should include the three EPR parameters a, D and $(a-F)$. The parameter a relates to a fourth-order spin operator and represents a cubic component of the crystalline electric field. The parameters D and $(a-F)$ relate to the axial ligand-field. So, generally speaking, the EPR parameters D and $(a-F)$ should be simultaneously considered in the determination of the local distortion structures for Fe^{3+} doped in crystals. In the present paper we study the crystal structure around an Fe^{3+} ion located at an octahedral site in $MgTiO_3$ and $LiTaO_3$ by simulating the EPR parameters D and $(a-F)$ simultaneously.

2. Theoretical Method

The perturbation Hamiltonian of an ion of d^5 configuration in a trigonal ligand-field can be expressed as [17]

$$\begin{aligned}\hat{H} &= \hat{H}_{\mathrm{ee}} + \hat{H}_{\mathrm{SO}} + \hat{H}_{\mathrm{LF}} \\ &= \sum_{i<j} \frac{e^2}{r_{i,j}} + \zeta \sum_i l_i s_i + \sum_i V_i,\end{aligned} \tag{1}$$

where the first term is the electron-electron repulsion interaction, the second one is the spin-orbit coupling

interaction, and the third one is the ligand-field interaction.

V_i is the potential function that may be expressed as

$$\begin{aligned} V_i = {} & \gamma_{00}Z_{00} + \gamma_{20}r_i^2 Z_{20}(\theta_i,\varphi_i) \\ & + \gamma_{40}r_i^4 Z_{40}(\theta_i,\varphi_i) + \gamma_{43}^c r_i^4 Z_{43}^c(\theta_i,\varphi_i) \\ & + \gamma_{43}^s r_i^4 Z_{43}^s(\theta_i,\varphi_i), \end{aligned} \tag{2}$$

where r_i, θ_i and φ_i are the spherical coordinates of the i-th electron. Z_{lm}, Z_{lm}^c and Z_{lm}^s are defined as

$$\begin{aligned} Z_{l0} = Y_{l0}, \quad Z_{lm}^c &= \left(1/\sqrt{2}\right)[Y_{l,-m} + (-1)^m Y_{l,m}], \\ Z_{lm}^s &= \left(\mathrm{i}/\sqrt{2}\right)[Y_{l,-m} - (-1)^m Y_{l,m}]. \end{aligned} \tag{3}$$

The $Y_{l,m}$ in (3) are the spherical harmonics. γ_{l0}, γ_{lm}^c and γ_{lm}^s are associated with the local structure around the d^5 configuration ion by the relations

$$\begin{aligned} \gamma_{l0} &= -\frac{4\pi}{2l+1}\sum_{i=1}^{n}\frac{eq_i}{R_i^{l+1}}Z_{l0}(\theta_i,\varphi_i), \\ \gamma_{lm}^c &= -\frac{4\pi}{2l+1}\sum_{i=1}^{n}\frac{eq_i}{R_i^{l+1}}Z_{lm}^c(\theta_i,\varphi_i), \\ \gamma_{l0}^s &= -\frac{4\pi}{2l+1}\sum_{i=1}^{n}\frac{eq_i}{R_i^{l+1}}Z_{lm}^s(\theta_i,\varphi_i), \end{aligned} \tag{4}$$

where θ_i and φ_i are the angular coordinates of the ligand, i and q_i represent the i-th ligand ion and its effective charge, respectively. R_i denotes the impurity-ligand distance.

Three 84×84 energy matrices for a d^5 configuration ion, corresponding to the perturbation Hamiltonian (1), have been derived, based on the irreducible representations $\Gamma 4(\Gamma 5)$ and $\Gamma 6$ of $C_3{}^*$ point group [17]. The matrix elements are functions of the Racah parameters B and C, Trees correction α, seniority correction β, the spin-orbit coupling coefficient ζ, and the ligand-field parameters B_{20}, B_{40}, B_{43}^c. For Fe^{3+} doped in $MgTiO_3$ crystal or $LiTaO_3$ crystal, the ligand-field parameters have the forms

$$\begin{aligned} B_{20} &= \frac{3}{2}\big[G_2(p_1)(3\cos^2\theta_1 - 1) \\ &\quad + G_2(p_2)(3\cos^2\theta_2 - 1)\big], \\ B_{40} &= \frac{3}{8}\big[G_4(p_1)(35\cos^4\theta_1 - 30\cos^2\theta_1 + 3) \\ &\quad + G_4(p_2)(35\cos^4\theta_2 - 30\cos^2\theta_2 + 3)\big], \\ B_{43}^c &= \frac{3}{4}\sqrt{35}\big[G_4(p_1)\cos\theta_1\sin^3\theta_1 \\ &\quad + G_4(p_2)\cos\theta_2\sin^3\theta_2\big], \end{aligned} \tag{5}$$

where

$$\begin{aligned} & G_2(p_i) = qeG^2(p_i), \quad G_4(p_i) = qeG^4(p_i), \\ & G^k(p_i) = \int_0^{R_{p_i}} R_{3d}^2(r)r^2\frac{r^k}{R_{p_i}^{k+1}}\mathrm{d}r \\ & \qquad + \int_{R_{p_i}}^{\infty} R_{3d}^2(r)r^2\frac{R_{p_i}^k}{r^{k+1}}\mathrm{d}r. \end{aligned} \tag{6}$$

We use p_1, p_2 to represent the ligand ions in the up and down pyramids in the $MgTiO_3$:Fe^{3+} or $LiTaO_3$:Fe^{3+} system and use θ_1, θ_2 to represent the corresponding angles between the metal-ligand bonds and the C_3 axis, respectively. Since the bond lengths in the octahedron in $MgTiO_3$:Fe^{3+} or $LiTaO_3$:Fe^{3+} are different [18], we may predict that

$$G_2(p_1) \neq G_2(p_2), \quad G_4(p_1) \neq G_4(p_2). \tag{7}$$

According to the Van Vleck approximation of the $G^k(p_i)$ integral [19], we can obtain the relations

$$G_2(P_i) = \frac{A_2}{{R_{P_i}}^3}, \quad G_4(P_i) = \frac{A_4}{{R_{P_i}}^5}, \tag{8}$$

where

$$A_2 = -eq_\tau\langle r^2\rangle,\ A_4 = -eq_\tau\langle r^4\rangle,\ A_2/A_4 = \langle r^2\rangle/\langle r^4\rangle.$$

The ratio of $\langle r^2\rangle/\langle r^4\rangle = 0.097$ is obtained from the radial wave function of Fe^{3+} in complexes [20]. A_4 as a constant for an octahedral $[FeO_6]^{9-}$ cluster can be determined from the optical spectra and the Fe-O bond length of the α-Fe_2O_3 crystal [21, 22]. In this way, we derive $A_4 = 27.6967$ au and $A_2 = 2.6870$ au for an octahedral $[FeO_6]^{9-}$ cluster, and we will take them in the following calculation.

The EPR spectra of a d^5 configuration Fe^{3+} ion in a trigonal ligand-field can be analyzed by employing the spin Hamiltonian [23, 24]

$$\hat{H}_S = \beta\vec{S}\cdot g\cdot\vec{B}_0 + \frac{1}{3}b_2^0O_2^0 + \frac{1}{60}(b_4^0O_4^0 + b_4^3O_4^3), \tag{9}$$

where b_k^q are the EPR zero-field splitting parameters and O_k^q are the standard Stevens spin operators. The O_k^q can be expressed as [24]

$$O_2^0 = 3S_z^2 - S(S+1),$$

$$O_4^0 = 35S_z^4 - 30S(S+1)S_z^2 + 25S_z^2 - 6S(S+1) + 3S^2(S+1)^2,$$
$$O_4^3 = 1/4[S_z(S_+^3 + S_-^3) + (S_+^3 + S_-^3)S_z]. \quad (10)$$

From the spin Hamiltonian, the splitting energy levels in the ground state $^6A_1$ for a zero magnetic field are given as [25, 26]

$$E_{\pm 1/2} = (1/3)b_2^0 + (3/2)b_4^0 \mp (1/6)[(18b_2^0 - 3b_4^0)^2 + (9/10)(b_4^3)^2]^{1/2},$$
$$E_{\pm 3/2} = -(2/3)b_2^0 - 3b_4^0, \quad (11)$$
$$E_{\pm 5/2} = (1/3)b_2^0 + (3/2)b_4^0 \pm (1/6)[(18b_2^0 - 3b_4^0)^2 + (9/10)(b_4^3)^2]^{1/2}.$$

Then, the zero-field splitting energies ΔE_1 and ΔE_2, which are energies between three Kramers doublets of the $^6A_1$ ground state, can be explicitly expressed as a function of the EPR parameters b_2^0, b_4^0, and b_4^3:

$$\Delta E_1 = (\pm 1/3)[(18b_2^0 - 3b_4^0)^2 + (9/10)(b_4^3)^2]^{1/2},$$
$$\Delta E_2 = -b_2^0 - (9/2)b_4^0 \pm (1/6)[(18b_2^0 - 3b_4^0)^2 + (9/10)(b_4^3)^2]^{1/2}. \quad (12)$$

The positive and negative signs in (12) correspond to $b_2^0 \geq 0$ and $b_2^0 < 0$, respectively. Here exists the simple relationship between the b_2^0, b_4^0, b_4^3 parameters and the EPR parameters D, a, $(a-F)$:

$$D = b_2^0, \quad a = -\frac{3}{20\sqrt{2}}b_4^3, \quad a - F = -3b_4^0.$$

Corresponding to the relation $D \gg a$, Kuang had shown that the low-symmetry EPR parameters D and $(a-F)$ are almost independent of the EPR cubic parameter a for Fe^{3+} in the Al_2O_3:Fe^{3+} system [17]. We note that this conclusion is also suitable for Fe^{3+} doped in $MgTiO_3$ and $LiTaO_3$ crystals. Therefore, we can fix the parameter a when we study the relationship between the low-symmetry EPR parameters D, $(a-F)$ and the local structure distortion in the $MgTiO_3$:Fe^{3+} or $LiTaO_3$:Fe^{3+} system. Meanwhile, the local distortion structures of Fe^{3+} doped $MgTiO_3$ and in $LiTaO_3$ crystals are determined by diagonalizing the complete energy matrices.

3. Calculations

The lattice structures of $MgTiO_3$ and $LiTaO_3$ crystals are similar to the trigonal one of Al_2O_3. When the Fe^{3+} ion is doped in $MgTiO_3$ or $LiTaO_3$ crystals, the local lattice structure displays a trigonal distortion. This can be described by use of the two parameters $\Delta\theta_1$ and $\Delta\theta_2$. Here we use an approximate relationship to evaluate the Fe-O bond lengths in $MgTiO_3$:Fe^{3+} and $LiTaO_3$:Fe^{3+}:

$$R_1 = R_{10} + \Delta R, \quad R_2 = R_{20} + \Delta R, \quad (13)$$

where $R_{10} = 2.19$ Å and $R_{20} = 2.04$ Å are the Mg-O bond lengths in $MgTiO_3$; $R_{10} = 2.12$ Å and $R_{20} = 1.89$ Å are the Ti-O bond lengths in $MgTiO_3$; $R_{10} = 2.307$ Å and $R_{20} = 2.041$ Å are the Li-O bond lengths in $LiTaO_3$. To our knowledge, no optical spectra data were reported for Fe^{3+} in $MgTiO_3$:Fe^{3+} and $LiTaO_3$:Fe^{3+} but one can estimate it from the spectra data of α-Fe_2O_3. Thus, the values of $\Delta R = -0.08$ Å for Fe^{3+} replacing Mg^{2+} and $\Delta R = 0.04$ Å for Fe^{3+} replacing Ti^{4+} in $MgTiO_3$:Fe^{3+} and $\Delta R = -0.17$ Å for Fe^{3+} replacing Li^+ in $LiTaO_3$ are determined approximately by fitting the optical spectra of α-Fe_2O_3 [27, 28]. Then in $MgTiO_3$:Fe^{3+} or $LiTaO_3$:Fe^{3+}, the angles between the Fe-O bonds and the C_3 axis can be written as

$$\theta_1 = \theta_{10} + \Delta\theta_1, \quad \theta_2 = \theta_{20} + \Delta\theta_2, \quad (14)$$

where θ_{10}, θ_{20} represent the angles between the M(Mg, Ti, Li)-O bond and the C_3 axis in the up and down pyramids of the host MO_6 octahedron. The trigonal ligand-field parameters $(B_{20}, B_{40}, B_{43}^c)$ are functions of the distortion parameters $\Delta\theta_1$ and $\Delta\theta_2$. In order to reduce the number of adjustable parameters and to reflect the effect of covalence, we take an average covalence factor N and use the following relations:

$$B = N^4 B_0, \quad C = N^4 C_0,$$
$$\alpha = N^4 \alpha_0, \quad \beta = N^4 \beta_0, \quad \zeta = N^2 \zeta_0, \quad (15)$$

where $B_0 = 1106$ cm^{-1}, $C_0 = 3922$ cm^{-1}, $\alpha_0 = 81$ cm^{-1}, $\beta_0 = -29$ cm^{-1}, $\zeta_0 = 470$ cm^{-1}, are the free ion parameters of Fe^{3+} [29]. Then, by diagonalizing the complete energy matrices, the optical and EPR spectra of the $MgTiO_3$:Fe^{3+} and $LiTaO_3$:Fe^{3+} systems can be simulated with use of the distortion parameters $\Delta\theta_1$, $\Delta\theta_2$ and the covalence factor N. As for Fe^{3+} in $MgTiO_3$:Fe^{3+} or in $LiTaO_3$:Fe^{3+}, here we take a typical covalence factor N $(N = 0.91)$ as found in MgO:Fe^{3+} [29]. In order to calculate accurately, a reasonable variation range of the covalence factor N $(0.91 \sim 0.92)$ has been employed in the calculation.

$\Delta\theta_1$ (deg)	$\Delta\theta_2$ (deg)	ΔE_1	ΔE_2	D	$(a-F)$
0.854	−0.82	7648.20	2715.57	1268	107
	−1.82	6279.37	2266.69	1040	111
	−2.82	4778.41	1774.37	789	116
	−3.82	3163.00	1243.48	519	121
	−4.82	1462.59	686.99	234	127
1.854	−0.82	7958.30	2822.88	1320	109
	−1.82	6597.98	2376.90	1093	114
	−2.82	**5107.88**	**1886.86**	**844**	**118**
	−3.82	3507.20	1361.20	577	123
	−4.82	1820.70	808.19	294	128
2.854	−0.82	8306.39	2943.31	1378	112
	−1.82	6958.20	2500.53	1153	116
	−2.82	5483.82	2016.11	907	121
	−3.82	3901.48	1495.90	642	125
	−4.82	2235.41	948.22	364	130
Expt. [5]		5107.48	1886.74	844	118

Table 1. Ground-state zero-field splittings ΔE_1, ΔE_2 and EPR parameters D and $(a-F)$ for Fe^{3+} occupying Mg^{2+} in $MgTiO_3$:Fe^{3+} as a function of the distortion angles $\Delta\theta_1$, $\Delta\theta_2$. Values are given in 10^{-4} cm^{-1} (except $\Delta\theta_1$, $\Delta\theta_2$), $N = 0.91$.

$\Delta\theta_1$ (deg)	$\Delta\theta_2$ (deg)	ΔE_1	ΔE_2	D	$(a-F)$
3.02	−3.68	7535.02	2711.22	1248	128
	−4.68	5927.89	2180.60	980	131
	−5.68	4224.82	1618.50	695	134
	−6.68	2454.61	1036.11	399	138
	−7.68	707.28	471.57	100	145
4.02	−3.68	7979.70	2861.90	1322	129
	−4.68	6400.99	2341.31	1058	133
	−5.68	**4727.82**	**1789.02**	**779**	**136**
	−6.68	2990.11	1215.29	488	139
	−7.68	1236.38	641.10	193	144
5.02	−3.68	8463.82	3027.80	1403	132
	−4.68	6917.00	2516.10	1144	135
	−5.68	5278.32	1973.61	871	137
	−6.68	3575.90	1411.82	586	140
	−7.68	1847.88	842.59	296	143
Expt. [8]		4727.83	1788.91	779	136

Table 2. Ground-state zero-field splittings ΔE_1, ΔE_2 and EPR parameters D and $(a-F)$ for Fe^{3+} occupying Ti^{4+} in $MgTiO_3$:Fe^{3+} as a function of the distortion angles $\Delta\theta_1$, $\Delta\theta_2$. Values are given in 10^{-4} cm^{-1} (except $\Delta\theta_1$, $\Delta\theta_2$), $N = 0.91$.

$\Delta\theta_1$ (deg)	$\Delta\theta_2$ (deg)	ΔE_1	ΔE_2	D	$(a-F)$
3.48	−4.621	19502.98	6739.50	3241.38	152.93
	−5.621	18980.90	6580.51	3153.82	162.58
	−6.621	18174.02	6328.39	3018.71	173.39
	−7.621	17082.02	5980.42	2836.10	183.67
	−8.621	15708.92	5539.13	2606.60	194.18
4.48	−4.621	19844.90	6864.40	3297.99	159.96
	−5.621	19324.91	6707.12	3210.74	170.26
	−6.621	**18516.88**	**6453.10**	**3075.49**	**180.10**
	−7.621	17420.92	6104.20	2892.21	190.63
	−8.621	16043.28	5661.20	2661.96	201.02
5.48	−4.621	20203.48	6995.39	3357.35	167.34
	−5.621	19690.82	6840.52	3271.32	177.62
	−6.621	18886.03	6588.02	3136.61	187.74
	−7.621	17791.86	6239.59	2953.62	198.18
	−8.621	16414.99	5795.90	2723.54	207.97
Expt. [15]		18516.70	6453.07	3075.46	180.12

Table 3. Ground-state zero-field splittings ΔE_1, ΔE_2 and EPR parameters D and $(a-F)$ for Fe^{3+} occupying Li^{+} in $LiTaO_3$:Fe^{3+} as a function of the distortion angles $\Delta\theta_1$, $\Delta\theta_2$. Values are given in 10^{-4} cm^{-1} (except $\Delta\theta_1$, $\Delta\theta_2$), $N = 0.91$.

The comparison between the theoretical values and the experimental data are listed in Tables 1–4.

From Tables 1–4, we can see that the experimental findings of the EPR parameters D and $(a-F)$ can be satisfactorily explained by the distortion parameters $\Delta\theta_1$ and $\Delta\theta_2$. The local distortion parameters $\Delta R = -0.08 \sim -0.098$ Å, $\Delta\theta_1 = 1.854 \sim 3.177°$, $\Delta\theta_2 = -2.82 \sim -3.17°$ for Fe^{3+} replacing Mg^{2+} in

Table 4. The EPR parameters D and $(a-F)$ for Fe^{3+} in $MgTiO_3$ and $LiTaO_3$:Fe^{3+} as a function of the covalence factor N, where ΔE_1, ΔE_2, D and $(a-F)$ are in units of 10^{-4} cm^{-1}.

	N	ΔR	$\Delta\theta_1$ (deg)	$\Delta\theta_2$ (deg)	ΔE_1	ΔE_2	D	$(a-F)$
$MgTiO_3$:Mg^{2+}	0.91	−0.08	1.854	−2.82	5107.88	1886.86	844	118
	0.915	−0.089	2.483	−2.98	5107.50	1886.79	844	118
	0.92	−0.098	3.177	−3.17	5107.50	1886.52	844	118
Expt. [5]					5107.48	1886.74	844	118
$MgTiO_3$:Ti^{4+}	0.91	0.04	4.02	−5.68	4727.82	1789.02	779	136
	0.915	0.03	4.282	−5.79	4727.48	1788.29	779	136
	0.92	0.02	4.747	−5.97	4727.40	1788.41	779	136
Expt. [8]					4727.83	1788.91	779	136
$LiTaO_3$:Li^{+}	0.91	−0.17	4.48	−6.621	18516.88	6453.10	3075.49	180.10
	0.915	−0.178	4.998	−6.748	18516.92	6453.10	3075.50	180.09
	0.92	−0.187	5.154	−6.901	18516.92	6453.10	3075.50	180.09
Expt. [15]					18516.70	6453.07	3075.46	180.12

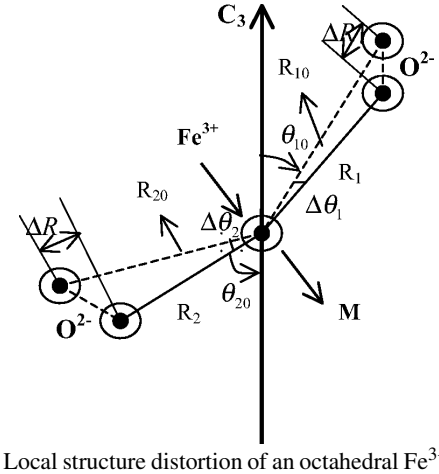

Fig. 1. Local structure distortion of an octahedral Fe^{3+} center in $MgTiO_3$ or $LiTaO_3$. M represents the Mg^{2+} or Li^{+} ion.

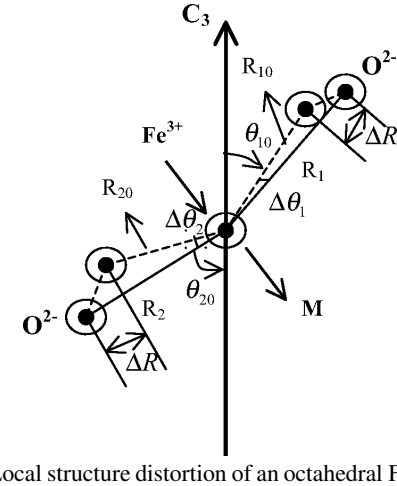

Fig. 2. Local structure distortion of an octahedral Fe^{3+} center in $MgTiO_3$. M represents the Ti^{4+} ion.

$MgTiO_3$; $\Delta R = 0.04 \sim 0.02$ Å, $\Delta\theta_1 = 4.02 \sim 4.747°$, $\Delta\theta_2 = -5.68 \sim -5.97°$ for Fe^{3+} replacing Ti^{4+} in $MgTiO_3$; $\Delta R = -0.17 \sim -0.187$ Å, $\Delta\theta_1 = 4.48 \sim 5.154°$, $\Delta\theta_2 = -6.621 \sim -6.901°$ for Fe^{3+} replacing Li^{+} in the $LiTaO_3$ system are determined. The results show that there exist two opposite effects in the MO_6:Fe^{3+} system. The first is that the local structures of Fe^{3+} replacing Mg^{2+} in $MgTiO_3$ and replacing Li^{+} in $LiTaO_3$ exhibit compression distortions as shown in Figure 1. This tendency is mainly due to the fact that the effective charge of Fe^{3+} is larger than that of Mg^{2+} and Li^{+}. The second result is that the local structure of Fe^{3+} replacing Ti^{4+} in $MgTiO_3$ exhibits an elongation distortion as shown in Figure 2. The physical reasons may be attributed to the fact that the radius and effective charge of Fe^{3+} are smaller than those of Ti^{4+} ($r_i = 0.68$ Å). Based on our calculated results, we may conclude that Fe^{3+} may occupy the Mg^{2+} or the Ti^{4+} site in the $MgTiO_3$:Fe^{3+} system, while Fe^{3+} will occupy the Li^{+} site rather than Ta^{5+} site in the $LiTaO_3$:Fe^{3+} system. The results are in consistent with the ENDOR and EPR experiments.

4. Conclusion

The local structures when Fe^{3+} is doped in $MgTiO_3$ and $LiTaO_3$ have been studied by diagonalizing the complete energy matrices and considering the second- and fourth-order EPR parameters D and $(a-F)$ simultaneously. It was shown that when Fe^{3+} replaces Mg^{2+} in $MgTiO_3$ and Li^{+} in $LiTaO_3$, the local lattice structure exhibits a compression; whereas, when Fe^{3+} replaces Ti^{4+} in $MgTiO_3$, the local lattice structure exhibits an extension. The local structure parameters $R_1 = 2.11 \sim 2.092$ Å, $R_2 = 1.96 \sim 1.942$ Å, $\theta_1 = 47.054 \sim 48.377°$, $\theta_2 = 60.98 \sim 60.63°$ for Fe^{3+} replacing Mg^{2+} and $R_1 = 2.16 \sim 2.14$ Å, $R_2 = 1.93 \sim 1.91$ Å, $\theta_1 = 51.02 \sim 51.747°$, $\theta_2 = 59.02 \sim 58.73°$ for Fe^{3+} replacing Ti^{4+} in $MgTiO_3$:Fe^{3+}; $R_1 = 2.137 \sim 2.12$ Å, $R_2 = 1.871 \sim 1.854$ Å, $\theta_1 = 47.52 \sim 48.194°$,

$\theta_2 = 65.959 \sim 65.679^\circ$ for Fe^{3+} replacing Li^+ in $LiTaO_3$:Fe^{3+} have been determined, respectively, and the EPR parameters D and $(a-F)$ can get a reasonable explanation.

Acknowledgements

This work was supported in part by the National Natural Science Foundation (No.10374068) and the Doctoral Education Fund of Education Ministry (No. 20050610011) of China.

[1] V. A. Trepakov, V. S. Vikhnin, S. Kapphan, L. Jastrabik, J. Licher, and P. P. Syrnikov, J. Lumin. **87–89**, 1126 (2000).
[2] R. I. Eglitis, E. A. Kotomin, G. Borstel, S. E. Kapphan, and V. S. Vikhnin, Compu. Mater. Sci. **27**, 81 (2003).
[3] P. Mialhe, A. Briguet, and A. Erbeia, Solid State Commun. **9**, 775 (1971).
[4] C. Vigreux, B. Deneuve, J. El Fallah, and J. M. Haussonne, J. Eur. Cera. Soc. **21**, 1681 (2001).
[5] A. F. M. Y. Haider and A. Edgar, J. Phys. C: Solid State Phys. **13**, 6239 (1980).
[6] H. Sothe, L. G. Rowan, and J. M. Spaeth, J. Phys.: Condens. Matter **1**, 3591 (1989).
[7] T. H. Yeom, J. Phys.: Condens. Matter **13**, 10471 (2001).
[8] W. C. Zheng, J. Phys. Chem. Solids **56**, 61 (1995).
[9] E. L. Carranza and R. T. Cox, J. Phys. Chem. Solids **40**, 413 (1979).
[10] J. Lino Vega, E. Carranza Lopez, and A. Valera, Solid State Commun. **33**, 729 (1980).
[11] S. C. Abrahams and J. L. Bernstein, J. Phys. Chem. Solids **28**, 1685 (1967).
[12] S. C. Abrahams, E. Buehler, C. Hamilton, and S. J. Laplaga, J. Phys. Chem. Solids **34**, 521 (1973).
[13] V. A. Vazhenin, V. B. Guseva, M. Y. Artyomov, R. K. Route, M. M. Fejer, and R. L. Byer, J. Phys.: Condens. Matter **15**, 275 (2003).
[14] S. Q. Fang, D. C. Ma, T. Zhang, F. R. Ling, and B. Wang, Optik **117**, 72 (2006).
[15] M. Loyo Menoyo, D. J. Keeble, Y. Furukawa, and K. Kitamura, J. Phys.: Condens. Matter **16**, 9047 (2004).
[16] E. Kratzig and R. Orlowski, Appl. Phys. **15**, 133 (1978).
[17] X. Y. Kuang, Phys. Rev. B **36**, 712 (1987).
[18] R. Hsu, E. N. Maslen, D. du Boulay, and N. Ishizawa, Acta Crystallogr. B **53**, 420 (1997).
[19] J. H. Van Vleck, J. Chem. Phys. **1**, 208 (1932).
[20] X. Y. Kuang, Q. Q. Gou, and K. W. Zhou, Phys. Lett. A **293**, 293 (2002).
[21] D. M. Sherman, Phys. Chem. Minerals **12**, 161 (1985).
[22] R. W. Gwyckoff, Crystal Structures 2, Chapter V, Interscience Publishers LTD, London 1965, p. 4.
[23] C. Legein, J. Y. Buzaré, and C. Jacoboni, J. Non-Cryst. Solids **184**, 160 (1995).
[24] C. Legein, J. Y. Buzaré, and C. Jacoboni, J. Solid State Chem. **121**, 149 (1996).
[25] H. H. Towner, Y. M. Kim, and H. S. Story, J. Chem. Phys. **56**, 3676 (1972).
[26] A. Darwish, D. Ila, D. B. Poker, and D. K. Hensley, Nucl. Instrum. Methods B **141**, 679 (1998).
[27] David M. Sherman, Phys. Chem. Minerals **12**, 161 (1985).
[28] L. A. Marusak, R. Messier, and W. B. White, J. Phys. Chem. Solids **41**, 981 (1980).
[29] X. Y. Kuang, W. Zhang, and I. Morgenstern-Badarau, Phys. Rev. B **45**, 8104 (1992).